

RSC Advances



This is an *Accepted Manuscript*, which has been through the Royal Society of Chemistry peer review process and has been accepted for publication.

Accepted Manuscripts are published online shortly after acceptance, before technical editing, formatting and proof reading. Using this free service, authors can make their results available to the community, in citable form, before we publish the edited article. This *Accepted Manuscript* will be replaced by the edited, formatted and paginated article as soon as this is available.

You can find more information about *Accepted Manuscripts* in the [Information for Authors](#).

Please note that technical editing may introduce minor changes to the text and/or graphics, which may alter content. The journal's standard [Terms & Conditions](#) and the [Ethical guidelines](#) still apply. In no event shall the Royal Society of Chemistry be held responsible for any errors or omissions in this *Accepted Manuscript* or any consequences arising from the use of any information it contains.

Enhanced photoelectrochemical and photocatalytic activity by $\text{Cu}_2\text{O}/\text{SrTiO}_3$ p-n Heterojunction via a facile deposition-precipitation technique

Chunbo Liu, Ping Li, Guoling Wu, Bifu Luo, Shuang Lin, Ao Ren, Weidong Shi*

School of Chemistry and Chemical Engineering, Jiangsu University, Xuefu Road 301, Zhenjiang, 212013, P. R. China.

*Corresponding author: Tel.: +86 511 8879 0187 fax. : +86 511 8879 1108
E-mail address: swd1978@ujs.edu.cn (W. Shi)

ABSTRACT

In our work, a new visible-light-driven photocatalyst $\text{Cu}_2\text{O}/\text{SrTiO}_3$ (C/S) heterojunction was firstly prepared by a simple, facile and effective method: deposition-precipitation technique. The photocatalyst of Cu_2O nanoparticle is only about 5 nm, and SrTiO_3 (STO) nanocube is about 50 nm, which modified by Cu_2O nanoparticles. The samples are used as photocatalysts for photodegrading tetracycline (TC) under visible light irradiation. The sample 9- $\text{Cu}_2\text{O}/\text{SrTiO}_3$ (9-C/S) heterojunction shows the highest TC degradation ratio (77.65%), which is owing to the photogenerated-electrons of Cu_2O nanoparticles moved from the conduction band of Cu_2O to that of SrTiO_3 , resulting in the separation of electrons and holes. This work not only shows a possibility for substituting low-cost Cu_2O nanoparticles for noble metals in the photocatalytic degradation but also exhibits a facile deposition-precipitation technique for synthesizing narrow/wide band gap photocatalysts.

Keywords: Photocatalytic, Cu_2O , SrTiO_3 , heterojunction, visible light

Introduction

Owing to the ability of decomposing organic pollutants completely and splitting water into oxygen and hydrogen under light irradiation, the photocatalysis has been widely used in green energy and environmental water treatment.¹⁻³ Currently, due to their outstanding properties, including chemical stability, strong oxidizing activity, corrosion resistance, and nontoxicity, photocatalytically active semiconductors with good prospects are TiO_2 , SrTiO_3 and ZnO etc.⁴⁻⁶ However, the wide band gap (3.2 eV) for SrTiO_3 corresponds to the low absorption of solar light. Therefore, to get rid of the harassment in practical applications, many methods have been developed on SrTiO_3 modification, for instance, noble metal deposition, metal or nonmetal ion doping, sensitization with organic polymers, and coupling with the other semiconductors.⁷⁻⁹

Many studies including experimental results and theoretical calculations have demonstrated that the heterojunction formed by TiO_2 and modified metal oxides contributes to the efficient separation of photo-generated electron-hole pairs, which prolong the lifetime of excited electrons and holes.¹⁰⁻¹² Among various photocatalysts, p-type Cu_2O represents an important kind of metal oxide. It has many advantageous characteristics, such as low cost, nontoxicity, unique optical, electrical properties and narrow band gap of 2.0 eV, for use in hydrogen production, sensors, superconductors, solar cells, and photocatalysis.¹³⁻¹⁶

While the narrow band gap contributes to its effective utilization of solar energy, its strong adsorption of molecular oxygen could scavenge photoelectrons, minimizing the electron-hole pair recombination on its surface. It had been reported that the valence and conduction bands of Cu_2O are both higher than those of TiO_2 , which thermodynamically favors the movement of excited electrons and holes between them and could subsequently enhance the separation of charge carriers to decrease their recombination.¹⁷⁻²⁰ Zhang et al. loaded polyhedral Cu_2O particles on TiO_2 nanotubes arrays through electrodeposition, and found significant improvement in the visible-light activity as compared to pure TiO_2 nanotubes.²¹ Besides, $\text{Cu}_2\text{O}/\text{TiO}_2$ heterojunction was reported to have the ability of storage of multi-electrons, which can be utilized for follow-up dark reactions.²²

Herein, owing to the similar valence and conduction band position between SrTiO_3 and TiO_2 , we introduce the C/S heterojunction. Dipika Sharma et al. have synthesized C/S photoelectrode, which used for hydrogen generation.²³ However, the morphology of Cu_2O is anomalistic, and the synthesis is much more complicated than our deposition-precipitation technique. To the best of our knowledge, there is no report in the literature about the preparation of C/S heterojunction by a simple, facile and effective method. In this work, for the first time, we successfully loaded Cu_2O nanoparticles (NPs) onto the surface of STO

nanocubes (NCs) through a facile deposition-precipitation technique. This method has the following advantages: (1) these Cu_2O NPs are uniformly dispersed on STO NCs; (2) heterojunction can form between STO NCs and Cu_2O NPs, which induces visible-light absorption and efficient separation of photo-generated electrons and holes. The heterojunctions exhibit much better efficiency on degradation of tetracycline (TC) under visible light irradiation comparing with pure STO NCs, Cu_2O NPs, which can be ascribed to the p-n junctions between STO NCs and Cu_2O NPs. This work not only shows a possibility for substituting low-cost Cu_2O NPs for noble metals in the photocatalytic degradation but also exhibits a facile deposition-precipitation technique for synthesizing narrow/wide band gap photocatalysts.

2. Experimental

2.1. Materials

Titania TiO_2 (P25) was purchased from Degussa (Germany). $\text{Sr}(\text{OH})_2 \cdot 8\text{H}_2\text{O}$, $\text{CuSO}_4 \cdot 5\text{H}_2\text{O}$, KOH, NaOH, L-ascorbic acid solution and ethanol were purchased from Aladdin (Shanghai, China). All the reagents are analytically grade and used without further purification and deionizer water is used in the study.

2.2. Catalysts synthesis

2.2.1 Synthesis of STO NCs: the STO NCs were prepared by a simple hydrothermal method: 3 mmol $\text{Sr}(\text{OH})_2 \cdot 8\text{H}_2\text{O}$ and 3 mmol TiO_2 were

mixed in 33.3 ml deionizer water with 2.1 g KOH under vigorous stirring, then the solution was transferred to a 50 ml Teflon-lined stainless steel autoclave hydrothermally treated in an air-flow electric oven at 150°C for 72h. After natural cooling, the white STO NCs was collected by centrifugation and washed with deionizer water and ethanol for several times, and then dried at 60°C in air for 12h.

2.2.2 Synthesis of C/S heterojunction: 0.1g STO NCs and a certain amount of $\text{CuSO}_4 \cdot 5\text{H}_2\text{O}$ was dissolved in 20 mL of 0.2 M NaOH solution under magnetic stirring. Then, 1.0 mL of 0.1 M L-ascorbic acid solution was added. C/S heterojunction were harvested by centrifuging and washed with distilled water and ethanol several times. The pure Cu_2O NPs were prepared totally the same without adding STO NCs.

2.3. Photocatalytic degradation of Tetracycline

Photocatalytic degradation of Tetracycline (TC) was performed as previous research works. 0.1 g photocatalysts were added to 100 mL of tetracycline solution (10mg/L). In order to clear up the impact of adsorption, prior to light illumination, the suspension was endlessly stirred in the dark for 30 min. A 150 W Xe lamp equipped with a filter to cut off light of wavelength <420 nm was used as the light source. At given time interval, 10 ml of the suspension was sampled and measured by the UV-vis spectrometer at the maximum absorbance (357 nm for TC).

$$TC_{DR} = \frac{A_0 - A_t}{A_0} \times 100\%$$

A_0 is the initial absorbance of TC when reached absorption equilibrium, while A_i is the absorbency after the sampling analysis.

3. Results and discussion

3.1. Morphology Structure of STO NCs Decorated with Cu_2O NPs

As shown in Fig.1a, due to the size of STO is about 50 nm and the samples have reunion, so we cannot observe the morphology structure of 9-C/S heterojunction from scanning electron microscopy (SEM) image; for comparison, transmission electron microscopy (TEM) provides insights into the structure of 9-C/S heterojunction. As shown in Fig. 1b, the Cu_2O NPs are uniformly dispersed on the surface of STO NCs (about 50 nm). The morphologies and structures of 9-C/S heterojunction is further studied by HRTEM (Fig. 1c). The lattice fringes in the pure STO image have an interplanar spacing $d=0.225$ nm, which perfectly corresponds to the (111) plane of STO, and the interplanar spacing $d=0.213$ nm is corresponded to the (200) plane of Cu_2O . From the HRTEM of 9-C/S heterojunction, the particle size of Cu_2O is about 5 nm.

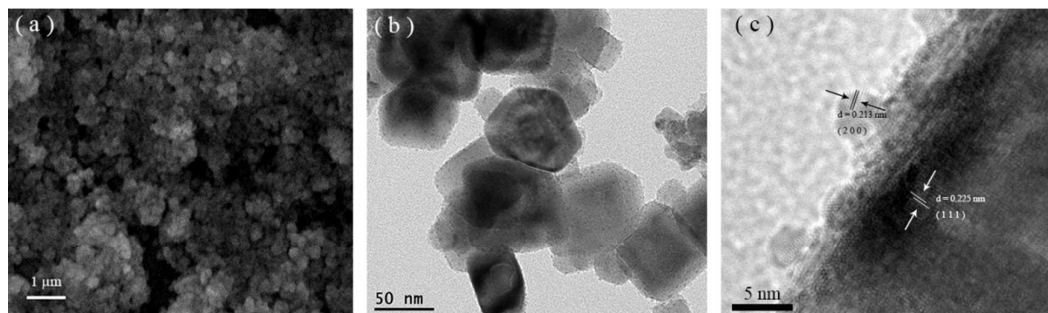


Fig. 1 SEM image of 9-C/S heterojunction (a); TEM image of 9-C/S heterojunction (b); HRTEM image of 9-C/S heterojunction (c).

3.2. Crystal Structure and Chemical Composition of STO NCs

Decorated with Cu₂O NPs

In order to investigate crystal phase composition, purity and element valence of the as-prepared samples, X-ray diffraction (XRD), energydispersive X-ray spectroscopy (EDX) and X-ray photoelectron spectroscopy (XPS) measurements were all carried out. The crystal structures of the samples were analyzed by XRD on a D/MAX-2500 X-ray powder diffractometer (Rigaku Corporation, Tokyo, Japan) with Cu K α ($\lambda = 1.54178 \text{ \AA}$) radiation at a scan rate of 5° min^{-1} . As shown in Fig. 2a, the all diffraction peaks observed at values of 22.8° , 32.2° , 40° , 46.5° , 58° , 68° and 77.2° of STO NCs (I) match that of the pure SrTiO₃ (JCPDS: 35-0734)⁷, and no other impurity peaks are detected, and it is also suitable for Cu₂O (II) (JCPDS: 05-0667)¹³, which implies high purity of as-prepared samples by our experimental strategies. EDX images were also collected on an F20 S-TWIN electron microscope (Tecnai G2, FEI Co.), using a 200 kV accelerating voltage. As displayed in Fig. 2b, the result of EDX gives the signals of Sr, Ti, O and Cu elements. XPS analysis was carried out by a Thermo ESCALAB 250X (America) electron spectrometer using 150 W Al K λ radiations. In Fig. 2c, XPS survey spectrum is carried out to demonstrate clearly the existence of Ti, O, and Cu in the sample. The emergence of the C element can be attributed to presence of carbon in the environment. Fig. 2d shows the

high resolution XPS scans over Cu 2p peak. The binding energies of Cu 2p_{3/2} and 2p_{1/2} are 932.5 and 952.8 eV, respectively, indicating that the sample contains Cu⁺ rather than Cu²⁺ (the characteristic peaks of Cu 2p_{3/2} for Cu(0), Cu(I), and Cu(II) are at 932 eV, 932.7 eV, and 933.6 eV, respectively).²⁴ The weak peaks shake up at about 942 eV in Fig. 2d is the shake-up peaks of Cu(II), this is because the chemical properties Cu₂O is instability, partial Cu₂O was oxidized to CuO. This can be ascribed to the relatively small amount and the amorphous nature of CuO that might be because of surface oxidization of Cu₂O.²⁵

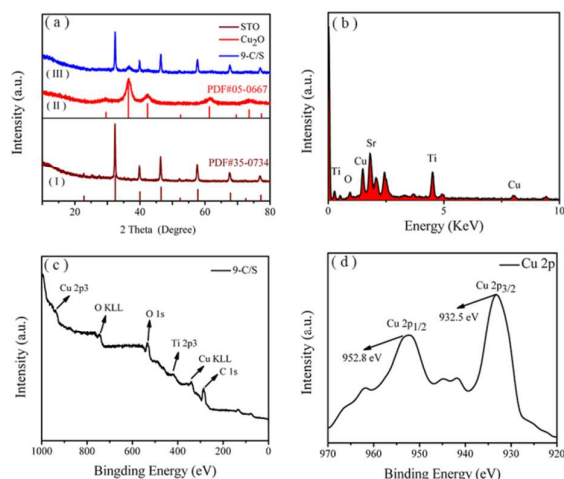


Fig. 2 (a) X-ray diffraction patterns of as-synthesized SrTiO₃ NCs (I), Cu₂O NPs (II) and Cu₂O/STO heterojunction (III); (b) energy dispersive X-ray spectroscopy of Cu₂O/STO heterojunction; (c) X-ray photoelectron spectroscopy survey spectrum of Cu₂O/STO heterojunction ; (d) The high resolution XPS scans over Cu 2p peak.

3.3. Optical Properties of STO NCs Decorated with Cu₂O NPs

The optical properties of these samples were investigated including

UV-vis diffuse reflectance spectra (UV-vis), electrochemical impedance spectroscopy (EIS) and photoresponse density. UV-vis of the as-prepared samples was obtained from a UV2550UV-vis spectrophotometer (Shimadzu, Japan) by using BaSO₄ as a reference. Fig. 3a shows the UV-vis/DR spectra of STO NCs, Cu₂O NPs and Cu₂O/STO heterojunction. Clearly, the absorption edge of pure STO is at approximately 400 nm, which agreed well with the band gap energy of STO NCs (E_g=3.2 eV). After coupling with of Cu₂O NPs, the Cu₂O/STO heterojunction show strong absorption both in UV and visible light, the absorption is even extended to larger than 500 nm, indicating this method can overcome the lack of visible light response of STO NCs.

In addition, another electrochemical analysis, EIS has also been done. As we all know, the impedance spectrum represents the degree of charge transfer and the relative higher separation of degree of the photogenerated electron/hole pair with the smaller size of radius of semicircle.²⁶ As shown in Fig. 3b, the radius of 9-C/S heterojunction is much smaller than that of the pure STO NCs, which means a more effective separation of photogenerated electron/hole pairs between the Cu₂O NPs and STO NCs surface.

Another interesting phenomenon is happened in the transient photocurrent of STO NCs and 9-C/S heterojunction under a visible light pulse of 30 s. As shown in Fig. 3c, firstly, the photocurrent was almost

measured to be zero in the dark; secondly, the photocurrent emerged without delay with the irradiation. Lastly, when the irradiation was suspended, the current apace fell to zero. It means that the sample is sensitive to the light. And the photocurrent density of 9-C/S heterojunction is roughly 4 times that of pure STO NCs, suggesting the excellent ability of electronic transmission and separation of photogenerated electron/hole pairs of 9-C/S heterojunction.²⁷

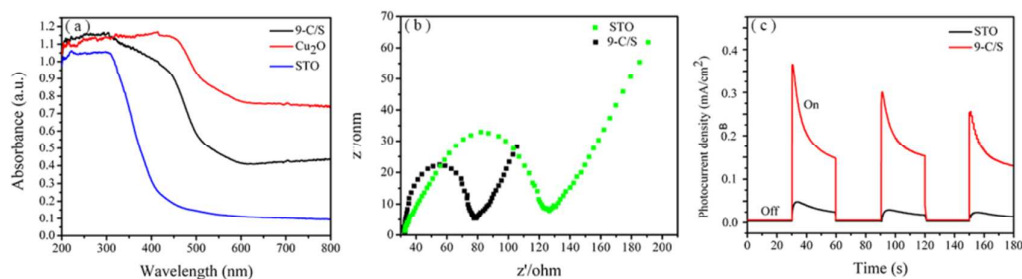


Fig. 3. (a) UV-vis diffuse reflectance spectra of STO NCs, Cu₂O NPs and 9-Cu₂O/STO heterojunction; (b) Electrochemical impedance spectroscopy spectra of pure SrTiO₃ NCs and 9-Cu₂O/STO heterojunction; (c) Photoresponse density of STO NCs and Cu₂O/STO heterojunction.

3.4. Photocatalytic Degradation of Tetracycline under Visible Light Illumination.

The photocatalytic abilities of as-prepared catalysts were certified by their photodegradation on a typical antibiotic pollutant, tetracycline, under visible light irradiation. As shown in Fig. 4a, the degradation of tetracycline can be neglected with the photocatalyst of STO NCs, owing to its wide band gap (3.2 eV), meanwhile the pure Cu₂O NPs exhibits a

degradation rate of only 21.42% under visible light irradiation. To surprise, combined with Cu₂O NPs, the C/S heterojunction show significant exaltation in the photodegradation of TC compared to pure STO NCs and Cu₂O NPs. The most predominant degradation ability could be obtained by using the 9 wt. % Cu₂O NPs loading one. This experimental result keep with that of UV-vis diffuse reflectance, and further confirm the truth that this method can enhance the photocatalytic activity of narrow/wide band gap photocatalysts.

In Fig. 4c, the linear relationship of $\ln(C_0/C)$ as a function of time implied that the photodegradation of TC followed an apparent first order kinetics, which can be calculated by $\ln(C_0/C) = kKt \approx k_{app}t$, where C_0 and C are the initial and reaction concentrations of TC, respectively. K_{app} represents the degradation rate constant and an index of photocatalytic ability, its value is proportional to the photocatalytic ability.⁷ So as shown in Fig. 4d, the K_{app} of photocatalytic degradation of TC by pure STO NCs and C/S heterojunction prepared by deposition of various amounts of Cu₂O NPs, were 0.00079, 0.0035, 0.0052, 0.0069, 0.013 and 0.010 min⁻¹, respectively. This value is consistent with the photocatalytic ability.

In order to determined the achievement is due to the photocatalysis instead of physical adsorption, total organic carbon (TOC) analyses were also conducted. TOC is a relevant parameter for the overall determination of the organic pollution of effluent and wastewaters. TOC analyses were

conducted on a multi N/C 2100 (Analytik Jena AG, Germany) TOC analyzer. As shown in Fig. 4e, the decomposition of TC with the photocatalyst of 9-C/S heterojunction under visible light is reached 47.6%, which is much lower than that of the photocatalysis. In Fig. 4f, similar trends of TOC removal and degradation curves indicate our photocatalysts have enormous potential of photodegrading antibiotics. Besides, it is also discovered that there still have a lot of other substances. In the test of optical properties and photocatalytic ability, we can draw a conclusion that this heterojunction can separate photogenerated electron/hole pairs and partly overcome the recombination of electrons and holes, thus excellently improve the photocatalytic ability.

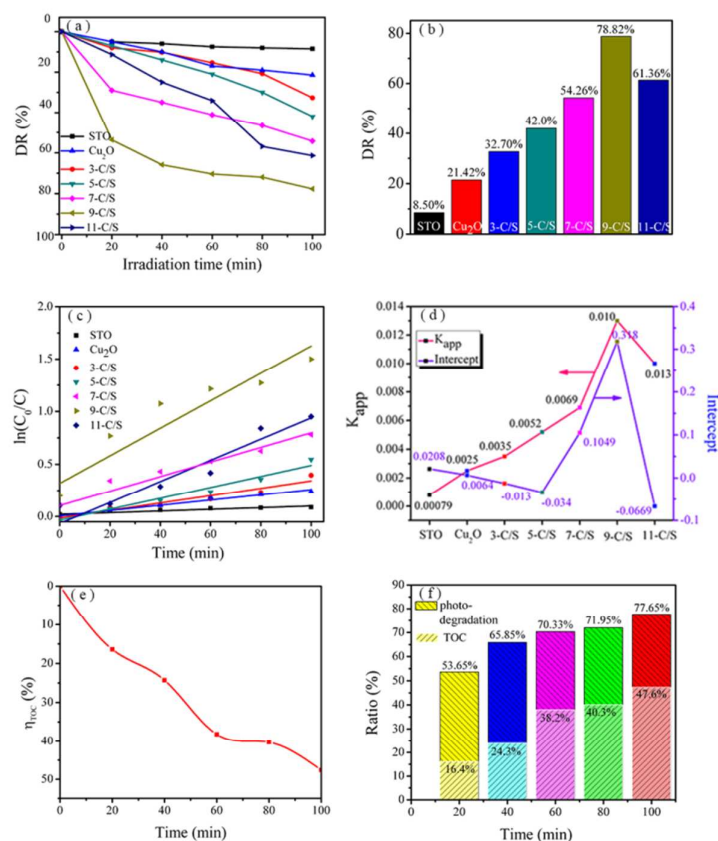


Fig. 4. (a) Photocatalytic degradation ratios of TC with different samples under visible light irradiation. (b) The pictorial diagram of photocatalytic degradation ratios of TC with different samples (c) The first-kinetic of the photocatalytic degradation of TC (d) Apparent rate constant values (pink color) and the intercept (purple color) for photodegradation of the TC solution over different photocatalysts in 140 min under visible light irradiation (e) TOC removal curves of 9-Cu₂O/STO heterojunction under visible light irradiation (f) Degradation curve trend contrasts tetracycline and TOC in 100 min.

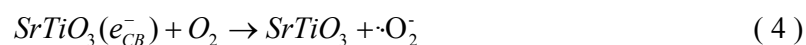
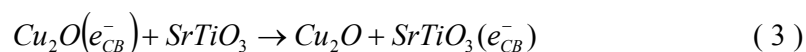
3.5. Mechanism on the Enhancement of Photocatalytic Activity of STO NCs Decorated with Cu₂O NPs

As we all know, all kinds of active species are heroes to photocatalytic, so in order to investigate the active species in our experiments, we conducted a series of active species trapping experiments: triethanolamine (TEA) is for h^+ ²⁸⁻³¹, iso-propanol (IPA) is for $\cdot OH$ ³¹ benzoquinone(BQ) is for $\cdot O_2^-$ ³⁰ and AgNO₃ is for e^- ²⁸⁻³¹ As shown in Fig. 5a-b, when IPA is added into the reaction system, the degradation ratio becomes 21.20%, suggesting $\cdot OH$ made a difference. A similar and obvious suppression phenomenon is also happened, the addition of AgNO₃ and BQ lead to 90% and 80% decrease to the photocatalytic degradation rate of TC under 9-C/S heterojunction, respectively. O₂ can be reduced by one electron into $\cdot O_2^-$, so the effect of addition of AgNO₃ is

similar to that of BQ. Conversely, the addition of TEA seems to be little effect on the photocatalytic activity. This result fully confirmed that these three active species promote the photodegradation, that are h^+ , $\cdot OH$ and $\cdot O_2^-$, besides $\cdot OH$ and $\cdot O_2^-$ play a main role in photocatalytic degradation system.

The generation of reactive species is further confirmed by an ESR technique with DMPO as a spin-trapping reagent in the visible-light-irradiation condition. Before the experiment, 10 mg photocatalysts were dissolved into 1 mL H_2O (CH_3OH) and 40 μL DMPO to form solution A: 9- Cu_2O /STO- H_2O -DMPO for detecting $\cdot OH$ (solution B: 9- Cu_2O /STO- CH_3OH -DMPO for detecting $\cdot O_2^-$). As shown in Fig. 5c, there are weak characteristic peaks assigned to DMPO- $\cdot OH$ adducts, which suggested that there are $\cdot OH$ reactive species generated. Meanwhile, the strong characteristic peaks with the peak area ratio are 1: 1: 1: 1: 1 are assigned to the DMPO- $\cdot O_2^-$ adducts shown in Fig. 5d, suggesting that the existence of $\cdot O_2^-$.⁷ This is because the photogenerated holes in the VB of Cu_2O NPs, and the photogenerated electrons in the CB of Cu_2O NPs will migrate to the CB of STO NCs. As a result, the photogenerated electrons and holes are accumulated in the CB of STO NCs and the VB of Cu_2O NPs, respectively. And owing to the positive E_{VB} of Cu_2O NPs (+0.46 V vs. NHE at pH = 0), the photogenerated h^+ in the VB of Cu_2O NPs cannot reduce OH^- into $\cdot OH$ with the redox potential

of +2.7 V vs. NHE at pH = 0, but the positive E_{BCB} (-0.3 V vs. NHE at pH = 0) of STO NCs, the photogenerated electrons in the CB of STO NCs can reduce O_2 into $\cdot\text{O}_2^-$ with the redox potential of -0.046 V vs. NHE at pH = 0.³³ However, $\cdot\text{O}_2^-$ can go to generate $\cdot\text{OH}$ with H_2O . Wherefore, combining the experimental results of active species trapping and ESR technique, we can conclude that the heroes of this exploration are $\cdot\text{OH}$ and $\cdot\text{O}_2^-$. As shown in Fig. 6, under visible irradiation, owing to the band gap, only the Cu_2O NPs can generate electron/hole pairs (reaction 2), the electrons can move from VB to CB of Cu_2O NPs, and further to the CB of STO NCs (reaction 3). As a result, the photogenerated electrons and holes are accumulated in the CB of STO NCs and the VB of Cu_2O NPs, respectively. The holes left in the VB of Cu_2O NPs are going to decompose TC directly. The electrons will react with O_2 to produce $\cdot\text{O}_2^-$ (reaction 4), portion of which will give birth to $\cdot\text{OH}$ (reaction 5, 6). The major electron transfer steps in the above photocatalytic mechanism under visible light irradiation are summarized by the following equations:



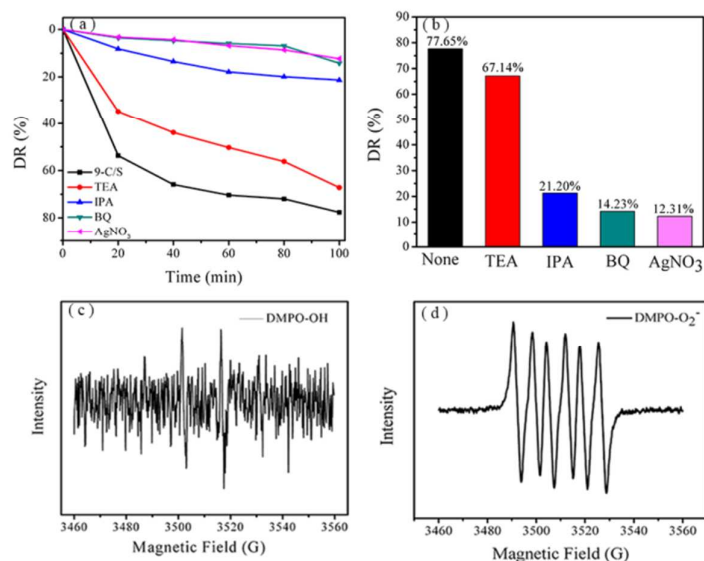


Fig.5. (a) Photocatalytic degradation ratios of TC using different radical scavengers over 9-Cu₂O/STO heterojunction under visible light irradiation for 100 min; (b) The pictorial diagram of photocatalytic degradation ratios of TC using different radical scavengers over 9-Cu₂O/STO heterojunction under visible light irradiation for 100 min; (c) DMPO spin-trapping ESR spectra of TC solutions after visible light irradiation by 9- Cu₂O/STO-H₂O-DMPO; (d) DMPO spin-trapping ESR spectra of TC solutions after visible light irradiation by 9- Cu₂O/STO-CH₃OH –DMPO.

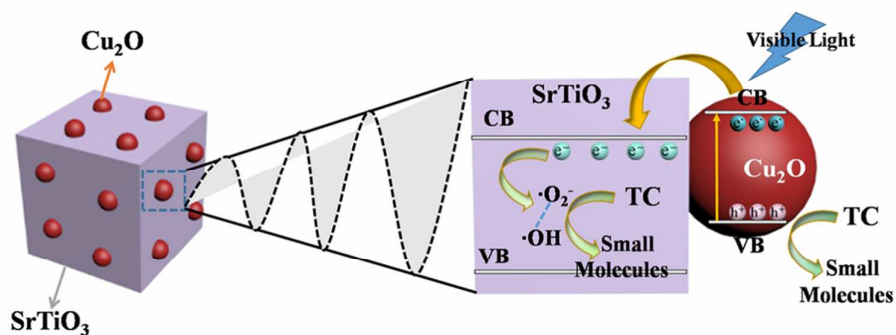


Fig.6. Mechanistic pathway of electrons and holes under visible light

illumination over 9-Cu₂O/STO heterojunction.

Conclusion

In summary, C/S heterojunction are synthesized for the first time via a facile deposition-precipitation technique. Compared to STO NCs and Cu₂O NPs, the prepared C/S heterojunction show perfect photodegradation of TC. The perfect Cu₂O NPs decorating content is about 9 wt. % and 9-C/S heterojunction had the best photocatalytic activity, reaching 77.65%, this is because the efficient separation of electrons and holes between Cu₂O NPs and STO NCs. This work not only shows a possibility for substituting low-cost Cu₂O nanoparticles for noble metals in the photocatalytic degradation but also exhibits a facile deposition-precipitation technique for synthesizing narrow band gap / wide band gap photocatalysts.

ACKNOWLEDGMENTS

The authors would like to acknowledge the National Natural Science Foundation of China (21276116, 21477050, 21301076, 21303074 and 21201085), the Excellent Youth Foundation of Jiangsu Scientific Committee (BK20140011, BK2012701), the Open Project of State Key Laboratory of Rare Earth Resource Utilizations (RERU2014010), the Program for New Century Excellent Talents in University

(NCET-13-0835), the Henry Fok Education Foundation (141068) and Six Talents Peak Project in Jiangsu Province (XCL-025).

REFERENCES

- (1) J. Zhi, S. Wenfeng, Rational removal of stabilizer-ligands from platinum nanoparticles supported on photocatalysts by self-photocatalysis degradation. *Catal. Today*, 2015, **242**, 372–380.
- (2) P. Meryem, M. S. Asli, A. Erdogan. Deniz, E. Huseyin, I. V. Evgeny, O. Emrah, Influence of the sol–gel preparation method on the photocatalytic NO oxidation performance of TiO₂/Al₂O₃ binary oxides. *Catal. Today*, 2015, **241**, 25–32.
- (3) C. B. Liu, D. S. Meng, Y. Li, L. L. Wang, Y. T. Liu, S. L. Luo, Hierarchical architectures of ZnS–In₂S₃ solid solution onto TiO₂ nanofibers with high visible-light photocatalytic activity. *J. Alloy. Compd.*, 2015, **624**, 44–52.
- (4) A. M. Ferrari-Lim, R. P. De Souza, S. S. Mendes, R. G. Marques, M. L. Gimenes, N.R.C. Fernandes-Machado, Photodegradation of benzene, toluene and xylenes under visible light applying N-doped mixed TiO₂ and ZnO catalysts. *Catal. Today*, 2015, **241**, 40–46.
- (5) C. B. Liu, L. L. Wang, Y. H. Tang, S. L. Luo,; Y. T. Liu, S. Q. Zhang, Y. X. Zeng,; Y. Z. Xu, Vertical single or few-layer MoS₂ nanosheets

rooting into TiO₂ nanofibers for highly efficient photocatalytic hydrogen evolution. *Appl. Catal. B-Environ*, 2015, **164**, 1–9.

(6) X. Y. Yue, J. Y. Zhang, F. P. Yan, X. Wang, F. Huang, A situ hydrothermal synthesis of SrTiO₃/TiO₂ heterojunction nanosheets with exposed (0 0 1) facets for enhancing photocatalytic degradation activity. *Appl. Surf. Sci.*, 2014, **319**, 68–74.

(7) P. Li, C. B. Liu, G. L. Wu, Y. Heng, S. Lin, A. Ren, K. H. Lv, L. S. Xiao, W. D. Shi, Solvothermal synthesis and visible light-driven photocatalytic degradation for tetracycline of Fe doped SrTiO₃. *RSC Adv.*, 2014, **4**, 47615-47624.

(8) X. Yan, S. F. Sun, B. Hu, X. Y. Wang, W. Lu, W. D. Shi, Enhanced photocatalytic activity induced by surface plasmon resonance on Ag-loaded strontium titanate nanoparticles. *Micro. Nano. Lett.*, 2013, **0452**, 1-4.

(9) X. J. Guan, L. J. Guo, Cocatalytic Effect of SrTiO₃ on Ag₃PO₄ toward Enhanced Photocatalytic Water Oxidation. *ACS Catal.*, 2014, **4**, 3020–3026.

(10) N. Michael, Surface modification of TiO₂ with metal oxide nanoclusters: a route to composite photocatalytic materials. *Chem. Commun.*, 2011, **47**, 8617–8619.

(11) T. Hiroaki, Q. L. Jin, N. Hiroaki, Y. Hironori, F. Musashi, O. Shin-ichi, H. Takanori, S. Yasutaka, K. Hisayoshi, Titanium(IV) Dioxide

Surface-Modified with Iron Oxide as a Visible Light Photocatalyst.

Angew. Chem. Int. Ed., 2011, **50**, 3501–3505.

(12) H. G. Yu, I. Hiroshi, S. Yoshiki, H. Yasuhiro, K. Yasushi, M. Masahiro, H. Kazuhito, An Efficient Visible-Light-Sensitive Fe(III)-Grafted TiO₂ Photocatalyst. *J. Phys. Chem. C*, 2010, **114**, 16481–16487.

(13) Y. Zhang, B. Deng, T. R. Zhang, D. M. Gao, A. W. Xu, Shape Effects of Cu₂O Polyhedral Microcrystals on Photocatalytic Activity. *J. Phys. Chem. C*, 2010, **114**, 5073–5079.

(14) X. X. Zhang, J. M. Song, J. Jiao, X. F. Mei, Preparation and photocatalytic activity of cuprous oxides. *Solid. State. Ssi.*, 2010, **12**, 1215-1219.

(15) J. Y. Ho, H. H. Michael, Synthesis of Submicrometer-Sized Cu₂O Crystals with Morphological Evolution from Cubic to Hexapod Structures and Their Comparative Photocatalytic Activity. *J. Phys. Chem. C*, 2009, **113**, 14159–14164.

(16) S. Z. Deng, T. Verawati, H. M. Fan, H. R. Tan, C. S. Dean, O. Malini, M. Subodh, W. Jun, H. S. Chornng, Reduced Graphene Oxide Conjugated Cu₂O Nanowire Mesocrystals for High-Performance NO₂ Gas Sensor. *J. Am. Chem. Soc.*, 2012, **134**, 4905–4917.

(17) D. D. Li, C. J. Chien, D. Suvil, P. C. Chang, M. Etienne, G. L. Jia, Prototype of a scalable core–shell Cu₂O/TiO₂ solar cell. *Chem. Phys. Lett.*,

2011, **501**, 446–450.

(18) D. Barreca, G. Carraro, A. Gasparotto, C. Maccato, M. Cruz-Yusta, J. L. Gómez-Camer, J. Morales, C. Sada, L. Sánchez, On the Performances of $\text{Cu}_x\text{O-TiO}_2$ ($x= 1, 2$) Nanomaterials As Innovative Anodes for Thin Film Lithium Batteries. *ACS Appl. Mater. Interfaces*, 2012, **4**, 3610–3619.

(19) R. Z. Ayib, T. Sakamoto, M. N. Uzer, R. Mohamad, M. Ichimura, New approach for generating $\text{Cu}_2\text{O/TiO}_2$ composite films for solar cell applications. *Mater. Lett.*, 2012, **66**, 254–256.

(20) L. Kannekanti, S. Gullapelli, D. K. Valluri, S. Machiraju, S. Bojja, Y. H. Neha, Highly Stabilized and Finely Dispersed $\text{Cu}_2\text{O/TiO}_2$: A Promising Visible Sensitive Photocatalyst for Continuous Production of Hydrogen from Glycerol:Water Mixtures. *J. Phys. Chem. C*, 2010, **114**, 22181–22189.

(21) J. Y. Zhang, H. L. Zhu, S. K. Zheng, F. Pan, T. M. Wang, TiO_2 Film/ Cu_2O Microgrid Heterojunction with Photocatalytic Activity under Solar Light Irradiation. *Adv. Mater.*, 2009, **10**, 2111–2114.

(22) J. P. Yasomanee, J. Bandara, Multi-electron storage of photoenergy using $\text{Cu}_2\text{O-TiO}_2$ thin film photocatalyst. *Sol. Energ. Mat. Sol C.*, 2008, **9**, 348–352.

(23) S. Dipika, U. Sumant, R. S. Vibha, S. Rohit, V. Umesh, S. D. Waghmare, Improved Photoelectrochemical Water Splitting Performance

of Cu₂O/SrTiO₃ Heterojunction Photoelectrode. *J. Phys. Chem. C*, 2014, **118**, 25320–25329.

(24) M.Y. Wang, L. Sun, Z. Q. Lin, J. H. Cai, K. P. Xie, C. J. Lin, p–n Heterojunction photoelectrodes composed of Cu₂O-loaded TiO₂ nanotube arrays with enhanced photoelectrochemical and photoelectrocatalytic activities. *Energy Environ. Sci.*, 2013, **6**, 1211–1220.

(25) X. Q. An, K. F. Li, J. W. Tang, Cu₂O/Reduced Graphene Oxide Composites for the Photocatalytic Conversion of CO₂. *ChemSusChem*, 2014, **7**, 1086 – 1093.

(26) C. Wang, J. C. Wu, P. F. Wang, Y. H. Ao, J. Hou, J. Qian, Photoelectrocatalytic determination of chemical oxygen demand under visible light using Cu₂O-loaded TiO₂ nanotube arrays electrode. *Sensor Actuat. B-Chem.*, 2013, **181**, 1–8.

(27) L. Zhao, W. Dong, F. G. Zheng, L. Fang, M. R. Shen, Interrupted growth and photoelectrochemistry of Cu₂O and Cu particles on TiO₂. *Electrochim Acta*, 2012, **80**, 354–361.

(28) L. Q. Ye, J. Y. Liu, C. Q. Gong, L. H. Tian, T. Y. Peng, L. Zan, Two Different Roles of Metallic Ag on Ag/AgX/BiOX (X = Cl, Br) Visible Light Photocatalysts: Surface Plasmon Resonance and ZScheme Bridge. *ACS Catal.*, 2012, **2**, 1677–1683.

(29) T. B. Li, G. Chen, C. Zhou, Z. Y. Shen, R. C. Jin, J. X. Sun, New photocatalyst BiOCl/BiOI composites with highly enhanced visible light

photocatalytic performances. *Dalton Trans.*, 2011, **40**, 6751–6758.

(30) S. C. Yan, Z. S. Li, Z. G. Zou, Photodegradation of Rhodamine B and Methyl Orange over Boron-Doped g-C₃N₄ under Visible Light Irradiation. *Langmuir*, 2010, **26(6)**, 3894–3901.

(31) X. N. Lu, Y. F. Ma, B. Z. Tian, J. L. Zhang, Preparation and characterization of FeTiO₂ films with high visible photoactivity by autoclaved-sol method at low temperature. *Solid. State. Ssi.*, 2011, **13**, 625-629.

(32) S. F. Chen, Y. F. Hu, L. Ji, X. L. Jiang, X. L. Fu, Preparation and characterization of direct Z-scheme photocatalyst Bi₂O₃/NaNbO₃ and its reaction mechanism. *Appl. Surf. Sci.*, 2014, **292**, 357–366.

(33) P. Zhou, J. G. Yu, J. Mietek, All-Solid-State Z-Scheme Photocatalytic Systems. *Adv. Mater.*, 2014, **26**, 4920–4935.